IEEE Access
Multidisciplinary | Rapid Review | Open Access Journal

Received 29 April 2024, accepted 8 May 2024, date of publication 14 May 2024, date of current version 24 May 2024.

Digital Object Identifier 10.1109/ACCESS.2024.3400939

RESEARCH ARTICLE

Low-Complexity MIMO Detection Based on DRSD With ISMMSE-PIC

SANG-SIK SHIN, HO JAE KIM, (Member, IEEE), AND HYOUNG-NAM KIM, (Member, IEEE)
Department of Electronics Engineering, Pusan National University, Busan 46241, Republic of Korea
Corresponding author: Hyoung-Nam Kim (hnkim@pusan.ac.kr)

This work was supported by the Brain Korea 21 Four (BK21FOUR), Creative Human Resource Education and Research Programs for Information and Communications Technology (ICT) Convergence in the 4th Industrial Revolution.

ABSTRACT This paper introduces a low-complexity multiple-input multiple-output (MIMO) detection method based on dimension-reduction-soft-demodulation (DRSD) with iterative soft minimum-mean-squared-error parallel interference cancellation (ISMMSE-PIC). The conventional ISMMSE-PIC detection method exhibits several drawbacks, such as inordinate dependence on decoder performance and modulation-order sensitivity. Therefore, a DRSD-based strategy is presented to search over a part of the set of transmitted symbols for calculating log-likelihood ratio (LLR) values, such as maximum likelihood detection, to improve detection performance. The scheme for the rest of the symbols directly utilizes ISMMSE-PIC detection for computing the corresponding LLR values. The computational complexity of the proposed scheme is similar to that of ISMMSE-PIC, whereas its bit error rate performance is comparatively higher. The complexity analysis and simulation results validate the proposed algorithm.

INDEX TERMS Multiple-input multiple-output, iterative soft minimum-mean-squared-error parallel interference cancellation, dimension reduction soft demodulation, geometric symmetry.

I. INTRODUCTION

multimedia data traffic of mobile users has soared since the invention of smartphones, portable multimedia devices, and tablet PCs. To meet the demand of the current explosive and continuous growth of data rate, advanced technologies, such as multiple-input multiple-output (MIMO) at the base station with a large number of antennas [1], [2], are required. The MIMO technology is considered as a main technology to provide a large network capacity and high spectral and energy efficiencies [3], [4]. It has been incorporated in numerous advanced wireless communication standards including the fifth generation (5G) communication systems and beyond. Concurrently, higher-order modulation, such as 256 quadrature amplitude modulation (QAM), has emerged as a standard for 5G communication systems [5], [6].

However, the MIMO approach is computationally complex owing to the inter-channel interferences between multiple antennas. Although the maximum likelihood (ML) detection is an optimal algorithm for uncoded MIMO systems, the associated computational complexity increases exponentially as the number of antennas increase [1], [7]. The common suboptimum MIMO detection schemes employ a linear zero-forcing (ZF) detector or various interference-cancellation-based detectors, such as minimum mean square error (MMSE), for hard-decision detection [8], [9]. However, channel coding, such as convolution or block coding, which results in correlation between bits, degrades the performance of suboptimum MIMO detectors. In coded systems, a soft-decision detector, which calculates the log-likelihood ratio (LLR) as reliability information of each bit, is used, instead of a hard-decision detector, to achieve a high performance [6]. Moreover, to secure high data rates, iterative detection and decoding (IDD) with a priori information is actively studied, with a focus on coded systems, owing to its high performance, which is better than that of non-iterative decoding in small-scale MIMO [10]. The IDD receivers transfer soft information, namely a priori information, between a detector and a channel decoder to achieve a near-optimal performance [11]. However, the computational

The associate editor coordinating the review of this manuscript and approving it for publication was Walid Al-Hussaibi.

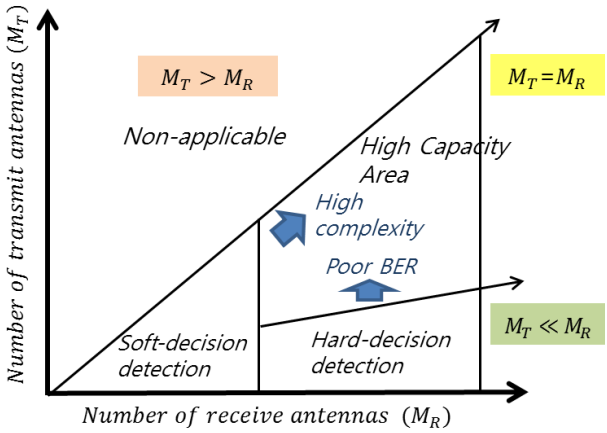

FIGURE 1. Feasibility area of MIMO through M_T and M_R.

complexity of IDD receivers surpasses that of non-IDD, and thus realizing their practical application in small-scale MIMO remains challenging. To overcome this limitation and reduce the computational complexity, dimension reduction algorithms, such as the sphere decoding algorithm [12], [13], and dimension-reduction soft demodulation (DRSD) with all ordering successive interference cancellation (AOSIC), have been introduced via hard-decision detection [14], [15]. The sphere decoder avoids an exhaustive search by examining only some points inside a sphere. DRSD searches over the part set of transmitted symbols to calculate the LLR values to reduce dimension. Transmitted symbols are partitioned into hard symbols and soft symbols. For the soft symbols, LLR values are computed. Following this computation, a process of dimension reduction is undertaken.

Fig. 1 shows the feasibility of MIMO systems depending on the number of receiver and transmitter antennas. In small-scale MIMO, soft-decision detection has better performance with practical computational complexity. In large-scale or massive MIMO, hard-decision detectors with channel hardening, which use more receiver antennas than the transmitter ones, exhibit high performance. Channel hardening implies that the channel approaches the deterministic limit, and the off-diagonal components become weaker compared to the diagonal terms as the size of the channel gain matrix increases [16]. Because of this property, simple matched filters (MFs) or MMSE are optimal for massive MIMO, and thus the classical complicated MIMO detection technology becomes redundant. However, this phenomenon occurs only with rich channel scattering and massive antenna arrays. Therefore, advanced detection techniques are required to expand the practicability of MIMO detection to high capacity areas, as shown in Fig. 1.

A. RELATED WORKS

As the number of antennas increases, channel-matrix-inversion calculations become infeasible because of the increased size and highly correlated channel matrix elements of the filtering vector. In addition, the cancellation of interference from other channels increases the computational complexity. To reduce the matrix inversion complexity, several approximate matrix inversion methods, such as the Neumann series expansion and Newton iteration method [17], [18], are employed. To minimize the inter-channel interferences, minimum-mean-squared-error parallel interference cancellation (MMSE-PIC) is required [19]. However, MMSE-PIC with mean and variance of symbols exhibits performance degradation in the absence of a priori information. Therefore, iterative soft MMSE-PIC (ISMMSE-PIC), which iteratively updates the mean and variance of the transmitted symbols by transferring a priori information between a detector and a channel decoder, is explored [20], [21], [22], [23].

B. PROBLEMS AND CONTRIBUTIONS

Notably, because of the reliance on suboptimal detectors such as MMSE, ISMMSE-PIC suffers from a significant degradation in its detection and is extremely sensitive to the modulation order owing to the decrease in spacing between the signal points of the modulation constellation. In addition, its iterative operation excessively relies on the channel decoder's performance [19], [20]. Therefore, to overcome these limitations, advanced detection algorithms, such as DRSD with AOSIC, are necessary. AOSIC with hard-decision detection is used for low-complexity SIC with different symbol orders [15]. Nevertheless, AOSIC, which is highly computationally complex, is not suitable for large-scale or massive MIMO systems because of the use of factorial candidates for hard-decision detection. Therefore, developing an efficient detection method with low complexity is essential. It initially presents the straightforward exchange of the AOSIC for MMSE-PIC for hard-decision detection. Although the performance of DRSD with MMSE-PIC surpasses that of ISMMSE-PIC, the computational complexity of the scheme is higher than that of ISMMSE-PIC. The reason is that the soft-decision procedure is recursively operated for the hard-decision detected symbols.

In this treatise, to reduce the complexity, a low-complexity MIMO detection method based on DRSD with ISMMSE-PIC is proposed. DRSD with MMSE-PIC is utilized to search over the part set of transmitted symbols for calculating the LLR values. By employing DRSD with MMSE-PIC to find hard-decision detected symbols, the proposed scheme for the rest of the symbols directly employs the ISMMSE-PIC detection method with the geometric symmetry property of the modulation constellation points. It enhances detection performance by utilizing partially DRSD MMSE-PIC detection. Because of improving initial detection performance, the proposed algorithm with iterative operation performs better than the ISMMSE-PIC detection as expected. To focus on

soft-decision detection, it is assumed that all the transmitted symbols have equal probability, and a priori information is not available as the first iteration.

C. PAPER ORGANIZATION

The remainder of this paper is organized as follows. Section II presents system model and reviews soft-decision detection and DRSD. Section III describes the proposed DRSD with MMSE-PIC. Complexity and performance evaluation are provided in Section IV. Finally, the conclusions are drawn in Section V.

D. NOTATIONS

Throughout the paper, the following notations are used. The superscripts $()^T$, $()^H$, and $()^{-1}$ represent the transpose, conjugate transpose, and inverse operations, respectively. $\mathbf{C}^{M\times N}$ is a set of all the complex matrices of size $M \times N$. *diag* stands for diagonal matrix. A_i is the i-th row of matrix A. M_T and M_R are the number of transmitter and receiver antennas, respectively. $M_R \geq M_T$ is assumed so that the rank deficient case, such as $M_R < M_T$, is not required to simplify the analysis. M represents the number of complex constellation points for modulation. n represents bits mapped to an M-ary modulation symbol with $M = 2^n$. P indicates the probability of an event, and its probability density function (pdf) is represented as p. $\lceil x \rceil$ represents ceiling operation.

II. SYSTEM MODEL AND DETECTION

A. SYSTEM MODEL

A coded spatially multiplexed (SM) MIMO system, wherein a transmitter with M_T transmitter antennas sends symbols to a receiver with M_R receiver antennas, is considered. $\mathbf{b}$ is transmitted data bit information, and the coded bits are represented by $\mathbf{x}$, which are encoded using a coding scheme, such as low density parity check, block codes, and turbo codes; $\mathbf{s}$ represent the transmitted symbols, which consist of n bits. Gray code mapping is used for bit-to-symbol mapping as shown in the upper part of Fig. 2; $\hat{\mathbf{s}}$ are the detected transmitted symbols, and $\hat{\mathbf{b}}$ are the estimated bits (shown in the lower part of Fig. 2); A group of M_T symbols is transmitted through multiple transmitter antennas, and the received signal vector $\mathbf{y}$ can be expressed as:

$$\mathbf{y} = \mathbf{H}\mathbf{s} + \mathbf{n}, \tag{1}$$

where $\mathbf{y} = [y_1 \ldots y_{M_R}]^T$ is an $(M_R \times 1)$ received signal vector, $\mathbf{s} = [s_1 \cdots s_{M_T}]^T$ is an $(M_T \times 1)$ transmitted symbol vector with s_m representing a transmitted symbol for m-th transmitter antenna. $\mathbf{H} = [\mathbf{h}_1 \ldots \mathbf{h}_{M_T}]$ is a $(M_R \times M_T)$ effective channel matrix with $\mathbf{h}_\mathrm{m}$ representing an $(M_R \times 1)$ channel gain vector from the m-th transmitter antenna to all the receiver antennas, and $\mathbf{n}$ is an $(M_R \times 1)$ noise vector. It is assumed that the noise is an independent, identically distributed circularly-symmetric complex Gaussian random vector with a covariance matrix $\sigma^2\mathbf{I}$. For simplicity, the time index is omitted, and the channel $\mathbf{H}$ and noise variance σ^2 are assumed to be perfectly known at the receiver end.

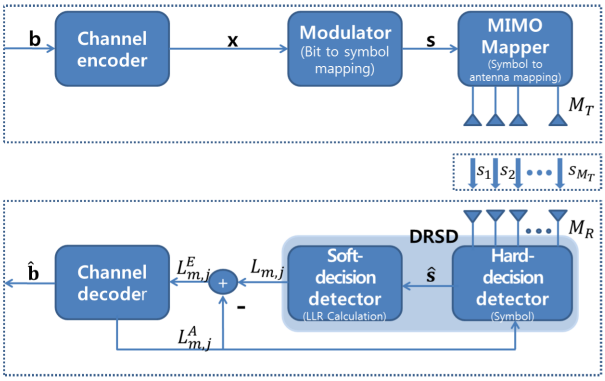

FIGURE 2. DRSD MIMO detection model.

B. SOFT-DECISION DETECTION AND DRSD

The MIMO soft-detection detector shown in Fig. 2 calculates $L_{m,j}$, which is the LLR of the j-th bit of the m-th transmitted symbol $\mathrm{b}_{m,j}$, according to the procedure demonstrated in [6]

$$L_{m,j} \triangleq \ln\left(\frac{\mathrm{P}[\mathrm{b}_{m,j}=1|\mathbf{y}]}{\mathrm{P}[\mathrm{b}_{m,j}=0|\mathbf{y}]}\right). \tag{2}$$

Following Bayes' theorem, (2) can be rewritten as:

$$L_{m,j} = \ln\left(\frac{\mathrm{P}(\mathbf{y}|\mathrm{b}_{m,j}=1)\mathrm{P}(\mathrm{b}_{m,j}=1)}{\mathrm{P}(\mathbf{y}|\mathrm{b}_{m,j}=0)\mathrm{P}(\mathrm{b}_{m,j}=0)}\right) \tag{3}$$

$$= \ln\left(\frac{\mathrm{P}(\mathrm{b}_{m,j}=1)}{\mathrm{P}(\mathrm{b}_{m,j}=0)}\right) + \ln\left(\frac{\mathrm{P}(\mathbf{y}|\mathrm{b}_{m,j}=1)}{\mathrm{P}(\mathbf{y}|\mathrm{b}_{m,j}=0)}\right) \tag{4}$$

$$= \ln\left(\frac{\mathrm{P}(\mathrm{b}_{m,j}=1)}{\mathrm{P}(\mathrm{b}_{m,j}=0)}\right) + \ln\left(\frac{\sum_{\mathbf{s}\in\mathbf{S}^1_{m,j}} \mathrm{p}(\mathbf{y}|\mathbf{s})}{\sum_{\mathbf{s}\in\mathbf{S}^0_{m,j}} \mathrm{p}(\mathbf{y}|\mathbf{s})}\right) \tag{5}$$

$$= L^A_{m,j} + L^E_{m,j} \tag{6}$$

for all the symbols $\mathbf{s} = 1, \ldots, M_T$ and all the bits b=1, …, n, where $\mathbf{S}^1_{m,j}$ and $\mathbf{S}^0_{m,j}$ are the sets of symbol vectors that have 1 and 0 at the j-th bit of the m-th symbol, respectively. $L_{m,j}$ can be divided into a priori information $L^A_{m,j}$ and extrinsic information $L^E_{m,j}$. As shown in Fig. 2, the extrinsic information is obtained by subtracting $L^A_{m,j}$ from $L_{m,j}$. For computational complexity reduction, the prior term $L^A_{m,j}$ is omitted. As shown in [24], this omitting does not result in a performance loss. The conditional pdf of the received signal vector $\mathbf{y}$ for a given transmitted symbol vector $\mathbf{s}$ is expressed as:

$$\mathrm{p}(\mathbf{y}|\mathbf{s}) = \frac{1}{(\pi\sigma^2)^{M_R}} \exp\left(-\frac{1}{\sigma^2}\|\mathbf{y}-\mathbf{H}\mathbf{s}\|^2\right). \tag{7}$$

As shown in Fig. 2, the $L_{m,j}$ values calculated by the detector are conveyed to a channel decoder. Max-log approximation is employed to reduce the complexity, although a slight

performance degradation is observed [6]; The approximate LLR can be defined as:

$$L_{m,j} = \ln\left(\sum_{\mathbf{s}\in\mathbf{S}^1_{m,j}} \exp\left(-\frac{1}{\sigma^2}\|\mathbf{y}-\mathbf{Hs}\|^2\right)\right) - \ln\left(\sum_{\mathbf{s}\in\mathbf{S}^0_{m,j}} \exp\left(-\frac{1}{\sigma^2}\|\mathbf{y}-\mathbf{Hs}\|^2\right)\right) \tag{8}$$

$$\approx \max_{s\in\mathbf{S}^1_{m,j}}\left\{-\frac{1}{\sigma^2}\|\mathbf{y}-\mathbf{Hs}\|^2\right\} - \max_{s\in\mathbf{S}^0_{m,j}}\left\{-\frac{1}{\sigma^2}\|\mathbf{y}-\mathbf{Hs}\|^2\right\} \tag{9}$$

$$\approx \min_{s\in\mathbf{S}^0_{m,j}}\left\{\frac{1}{\sigma^2}\|\mathbf{y}-\mathbf{Hs}\|^2\right\} - \min_{s\in\mathbf{S}^1_{m,j}}\left\{\frac{1}{\sigma^2}\|\mathbf{y}-\mathbf{Hs}\|^2\right\}. \tag{10}$$

To determine the LLR value for each bit, as observed in (10), M^{M_T} Euclidean distances (EDs) per LLR value are computed, which results in massive computational complexity at the detector end. DRSD, in which the transmitted symbols are divided into two groups, is introduced to calculate the LLR value of (10). For the soft-decision part of the transmitted symbols, the minimum ED is calculated as soft-decision detection, and the rest of the symbols employ hard-decision detection to determine the best transmitted symbol subvector.

The transmitted symbol vectors corresponding to the soft-detection symbols and remaining hard-detection symbols are represented as $\mathbf{s}^{so}$ and $\mathbf{s}^{ha}$, respectively. Then, a transmitted symbol vector can be divided as:

$$\mathbf{s} = \begin{bmatrix}\mathbf{s}^{ha}\\ \mathbf{s}^{so}\end{bmatrix}. \tag{11}$$

The channel matrix is also divided into two submatrices as:

$$\mathbf{H} = \begin{bmatrix}\mathbf{H}^{ha} & \mathbf{H}^{so}\end{bmatrix}, \tag{12}$$

where $\mathbf{H}^{ha} \in \mathbf{C}^{M_R\times M_T^{ha}}$ and $\mathbf{H}^{so} \in \mathbf{C}^{M_R\times M_T^{so}}$ represent the channel matrices for $\mathbf{s}^{ha}$ and $\mathbf{s}^{so}$, respectively. The received signal is represented as:

$$\mathbf{y} = \mathbf{H}^{ha}\mathbf{s}^{ha} + \mathbf{H}^{so}\mathbf{s}^{so} + \mathbf{n}. \tag{13}$$

The LLR in (10), wherein the m-th symbol represents one of the M_T^{so} soft symbols, is transformed as:

$$L_{m,j} = \min_{\mathbf{s}^{so}\in\mathbf{S}^{so(0)}_{m,j},\,\mathbf{s}^{ha}\in\mathbf{S}^{ha}}\left\{\frac{1}{\sigma^2}\left\|\mathbf{y}-\mathbf{H}^{ha}\mathbf{s}^{ha}-\mathbf{H}^{so}\mathbf{s}^{so}\right\|^2\right\} - \min_{\mathbf{s}^{so}\in\mathbf{S}^{so(1)}_{m,j},\,\mathbf{s}^{ha}\in\mathbf{S}^{ha}}\left\{\frac{1}{\sigma^2}\left\|\mathbf{y}-\mathbf{H}^{ha}\mathbf{s}^{ha}-\mathbf{H}^{so}\mathbf{s}^{so}\right\|^2\right\}, \tag{14}$$

where $\mathbf{S}^{so(b)}_{m,j}$ is the set of soft-detection transmitted symbol subvectors $\mathbf{s}^{so}$ with $b_{m,j} = b$ of the m-th symbol, and $\mathbf{S}^{ha}$ is the set of all hard-detection transmitted symbol subvectors $\mathbf{s}^{ha}$. Notably, (14) can be represented as an optimization problem, composed of hard and soft symbol decisions for the sets $\mathbf{S}^{so(b)}_{m,j}$ and $\mathbf{S}^{ha}$, in two steps as : 1) for each $\mathbf{s}^{so}$, identify the minimum ED over the set $\mathbf{S}^{ha}$, 2) calculate the minimum ED of each $\mathbf{s}^{so}$ as

$$L_{m,j} = \min_{\mathbf{s}^{so}\in\mathbf{S}^{so(0)}_{m,j}}\left\{\min_{\mathbf{s}^{ha}\in\mathbf{S}^{ha}}\left[\frac{1}{\sigma^2}\left\|\mathbf{y}(\mathbf{s}^{so})-\mathbf{H}^{ha}\mathbf{s}^{ha}\right\|^2\right]\right\} - \min_{\mathbf{s}^{so}\in\mathbf{S}^{so(1)}_{m,j}}\left\{\min_{\mathbf{s}^{ha}\in\mathbf{S}^{ha}}\left[\frac{1}{\sigma^2}\left\|\mathbf{y}(\mathbf{s}^{so})-\mathbf{H}^{ha}\mathbf{s}^{ha}\right\|^2\right]\right\}, \tag{15}$$

where

$$\mathbf{y}(\mathbf{s}^{so}) \triangleq \mathbf{y} - \mathbf{H}^{so}\mathbf{s}^{so}. \tag{16}$$

In (16), $\mathbf{y}(\mathbf{s}^{so})$ is formed by subtracting the term, originating from the soft symbols $\mathbf{s}^{so}$, from the received signal $\mathbf{y}$; this implies that after dividing into soft and hard symbols, Step 1 attempts to select the best hard symbols $\mathbf{s}^{ha}$ for a given $\mathbf{s}^{so}$, i.e., $\hat{\mathbf{s}}^{ha}(\mathbf{s}^{so})$, as

$$\hat{\mathbf{s}}^{ha}(\mathbf{s}^{so}) = \underset{\mathbf{s}^{ha}\in\mathbf{S}^{ha}}{\operatorname{argmin}}\left(\frac{1}{\sigma^2}\left\|\mathbf{y}(\mathbf{s}^{so})-\mathbf{H}^{ha}\mathbf{s}^{ha}\right\|^2\right). \tag{17}$$

For each $\mathbf{s}^{so}$, AOSIC can directly find vector $\bar{\mathbf{s}}^{ha}$ from the received signal [15].

$$\hat{\mathbf{s}}^{ha}(\mathbf{s}^{so}) = \underset{\bar{\mathbf{s}}^{ha}\in\Phi}{\operatorname{argmin}}\left(\frac{1}{\sigma^2}\left\|\mathbf{y}(\mathbf{s}^{so})-\mathbf{H}^{ha}\bar{\mathbf{s}}^{ha}\right\|^2\right), \quad \Phi = \{\bar{\mathbf{s}}^{ha}_1, \bar{\mathbf{s}}^{ha}_2, \cdots, \bar{\mathbf{s}}^{ha}_{(M_T^{ha})!}\} \tag{18}$$

where $\bar{\mathbf{s}}^{ha}_q$ is the output from the successive interference cancellation (SIC) with the q-th ordering, q=1,...,$(M_T^{ha})!$. To detect soft decisions for all transmitted symbols, the DRSD operation should be used recursively. LLR values for the remaining symbols can be calculated by rearranging the transmitted symbol vector.

To replace the AOSIC operation, a low-complexity MMSE-based receiver with parallel interference cancelation (PIC) for hard-decision detection is considered. This operation separates each symbol and cancels the interference of the other symbols with the mean and variance; the details are provided in the subsequent section.

III. PROPOSED DRSD WITH MMSE-PIC

Let $\bar{s}^{ha}_m$ and v^{ha}_m be the mean and variance of the transmitted symbol, respectively, for s^{ha}_m, and are calculated using the following equation:

$$\bar{s}^{ha}_m = \sum_{s\in\Omega} s\mathrm{P}(s) \tag{19}$$

and

$$v_m^{ha} = \sum_{s\in\Omega} \left| s - \bar{s}_m^{ha} \right|^2 \mathrm{P}(s), \tag{20}$$

where $\mathrm{P}(s_m = s) = \prod_{j=1}^{n} \mathrm{P}(s_{m,j} = b)$ denotes a priori probability of the symbol $s \in \Omega$ (a set of M constellation points), and $b = s_j$ is the b-th bit associated with the symbol s [21]. Before the first iteration, $\bar{s}_m^{ha}$ and v_m^{ha} are initialized as 0 and 1, respectively, resulting in an initial poor performance of ISMMSE-PIC without a priori information. After the first iteration, $\bar{s}_m^{ha}$ and v_m^{ha} can be updated with the a priori information, and the transmitted symbols do not have equal probabilities. Then, to detect s_m^{ha}, the $M_T \times 1$ hard-interference-cancelled vector $y_m(s^{so})$ can be calculated as

$$y_m(s^{so}) = \mathbf{y}(s^{so}) - \sum_{i=1, i\neq m}^{M_T^{ha}} h_i^{ha} \bar{s}_i^{ha}. \tag{21}$$

The $M_T^{ha} \times 1$ filtering vector w_m for s_m^{ha} is calculated as

$$w_m = (A_m^{ha})^{-1} h_m, \tag{22}$$

where

$$A_m^{ha} = \mathbf{H}^{ha} V_m H^{ha,H} + \sigma^2 I_m \tag{23}$$

$$V_m = diag([v_1, \cdots, v_m = 1, \cdots, v_{M_T^{ha}}]). \tag{24}$$

Calculating the filtering vector requires channel matrix inversion, which is repeated for estimating each transmitted symbol. To lower the complexity, all the M_T^{ha} MMSE filter vectors are computed solely via single-matrix inversion as [20]:

$$W = (A^{ha})^{-1} H^{ha}, \tag{25}$$

where

$$A^{ha} = \mathbf{H}^{ha} V^{ha} H^{ha,H} + \sigma^2 I \tag{26}$$

$$V^{ha} = diag([v_1, \cdots, v_{M_T^{ha}}]). \tag{27}$$

The rows w_m of $\mathbf{W}$ correspond to the MMSE filter vectors in (22). This proof is based on the Sherman–Morrison–Woodbury formula, which is expressed as: $(A + ab^H)^{-1} = A^{-1} - (A^{-1}abA^{-1})/(1 + b^H A^{-1} a)$ for a nonsingular matrix $\mathbf{A} \in \mathbf{C}^{M_R^{ha} \times M_T^{ha}}$ with $M_R^{ha} \times 1$ vectors $\mathbf{a}$ and $\mathbf{b}$. Because the second term of the formula is a constant, scaling w_m does not impact the distance indicated in (29). Then, the decision $\bar{s}_m^{ha}$ is calculated as:

$$\bar{s}_m^{ha} = \underset{\mathbf{s}\in\Omega}{\operatorname{argmin}} \left(\left| \breve{s}_m^{ha} - w_m^H h_m s \right|^2 \right), \tag{28}$$

where

$$\breve{s}_m^{ha} = w_m^H y_m(s^{so}). \tag{29}$$

An example of the MMSE-PIC detection algorithm is depicted in Fig. 3. Finally, the minimum ED for each $\mathbf{s}^{so}$ can be calculated based on (18) as:

$$\hat{\mathbf{s}}^{ha}(\mathbf{s}^{so}) = \frac{1}{\sigma^2} \left\| \mathbf{y}(\mathbf{s}^{so}) - \mathbf{H}^{ha} \bar{\mathbf{s}}^{ha}(\mathbf{s}^{so}) \right\|^2, \tag{30}$$

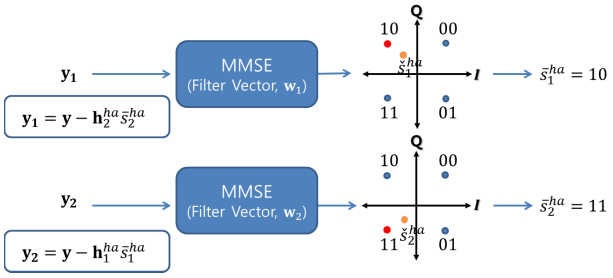

FIGURE 3. An example of MMSE-PIC detection algorithm.

where

$$\bar{\mathbf{s}}^{ha}(\mathbf{s}^{so}) = \{\bar{s}_1^{ha}, \bar{s}_2^{ha}, \cdots, \bar{s}_{M_T^{ha}}^{ha}\}. \tag{31}$$

However, to calculate the complete LLR values of all the transmitted symbols, the MMSE-PIC operation is used recursively, which in turn increases the computational complexity, and thus, this process is not feasible for systems with large antennas. To reduce the complexity, ISMMSE-PIC for hard symbols is directly employed for calculating the LLR values, and DRSD MMSE-PIC for soft symbols is utilized. The LLR values for soft symbols are initially calculated using (15), and we can identify $\hat{\mathbf{s}}_{min}^{ha}$, which has the minimum ED for $\mathbf{s}^{so}$ using the following equation:

$$\hat{\mathbf{s}}_{min}^{ha}\left(\mathbf{s}_{min}^{so}\right) = \min_{\mathbf{s}^{so}\in\mathbf{S}^{so}} \left\{ \frac{1}{\sigma^2} \left\| \mathbf{y}(\mathbf{s}^{so}) - \mathbf{H}^{ha} \bar{\mathbf{s}}^{ha}\left(\mathbf{s}^{so}\right) \right\|^2 \right\}, \tag{32}$$

where $\mathbf{S}^{so}$ is the set of soft-detection transmitted symbol subvectors $\mathbf{s}^{so}$. Because MMSE-PIC is incorporated for hard detection, ISMMSE-PIC is easily implemented to calculate the LLR values of the hard symbols as shown below:

$$L_{m,j}^{ha} = \min_{s\in\Omega_{\mathbf{j}}^0} \left\{ \frac{1}{\sigma^2} |\breve{s}_{min,m}^{ha} - w_m^H h_m s|^2 \right\} - \min_{s\in\Omega_{\mathbf{j}}^1} \left\{ \frac{1}{\sigma^2} \left| \breve{s}_{min,m}^{ha} - w_m^H h_m s \right|^2 \right\}, \tag{33}$$

where $\breve{s}_{min,m}^{ha}$ is the estimated symbol and is given by

$$\breve{s}_{min,m}^{ha} = w_m^H y_m(s_{min}^{so}). \tag{34}$$

Further, $\Omega_{\mathbf{j}}^0$ and $\Omega_{\mathbf{j}}^1$ are the sets of constellation points that have 0 and 1 at the j-th bit of each symbol, respectively. The proposed scheme can be easily extended to IDD, and the mean and variance of the transmitted symbols can be updated, owing to the incorporation of ISMMSE-PIC.

In summary, the proposed scheme extracts LLR^{so} and LLR^{ha} via DRSD MMSE-PIC and from ISMMSE-PIC detection, respectively. Moreover, the scheme delivers a remarkable initial performance without a priori information because of the implementation of soft detection for each constellation with M_T^{ha} MMSE filter vectors. Because of improving initial detection performance, the proposed scheme with iterative operation has showed better performance. ISMMSE-PIC detection for the hard symbols

TABLE 1. Key characteristics of the algorithms.

Algorithm	Differences and limitations
ML	· Optimal detection algorithm · High computational complexity
ISMMSE-PIC	· Suboptimal detection algorithm · Inordinate dependence on decoder performance
DRSD MMSE-PIC	· ML for soft-detection symbols · MMSE-PIC for hard-detection symbols · Recursive soft-decision for hard-detection symbols
Proposed	· DRSD MMSE-PIC for soft-detection symbols · ISMMSE-PIC for hard-detection symbols
Performance: ML > DRSD MMSE-PIC > Proposed > ISMMSE-PIC Complexity: ML > DRSD MMSE-PIC > ISMMSE-PIC ≈ Proposed	

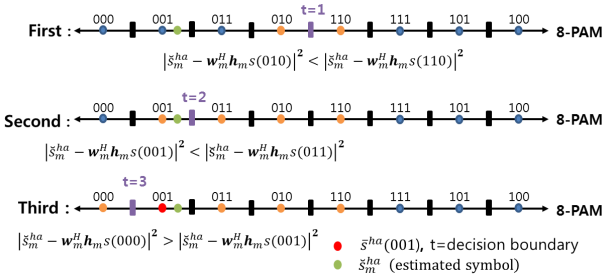

FIGURE 4. Algorithm of eight PAM geometric symmetry detection.

facilitates low-complexity calculation of LLR values, and IDD, which iteratively transfers the a priori information between the detector and decoder, is simply implemented to update the probabilities of the hard symbols. Depending on the channel and signal-to-noise ratio (SNR) conditions, the numbers of soft and hard symbols can be determined and optimal performances are achieved under diverse conditions. In conditions where the channel is mild and the SNR is high, there is an implementation of an increase in the use of hard symbols. Conversely, as the conditions become more adverse, there is a shift towards increasing the presence of soft symbols. Table 1 compares the key characteristics of the algorithms to highlight their differences and limitations.

Moreover, when higher-order QAM constellations are employed, the computational complexity of MMSE-PIC for hard detection amplifies because of the calculation of $\bar{s}_m^{ha}$ for the constellation points at each symbol using (29). To relieve the computational burden, a geometric symmetry property of the Gray coded modulation constellations is proposed; this property utilizes decision boundaries as $B = \{t_1, \ldots, t_n \mid n = log_2 M)\}$ [25], [26]. Fig. 4 illustrates an example of eight pulse amplitude modulation (PAM) symbols, and the decision boundaries at the j-th calculation step are denoted by t_j. Once the initial sequence is set, t_1 is selected as the center of the decision boundaries. Because of the symmetry of the initial decision boundary sequence, t_1 is always equal to 0 in the first step shown in Fig.4. The selection of t_2 and t_3 is followed by calculating the minimum distance for the next constellation points. Then, the calculation of (29) is reduced by a half + 1 of the constellation points. Because QAM can be decomposed into two independent (in phase and quadrature phase) PAMs, the individual QAM for the two PAMs can be easily calculated. Notably, the computational complexity is reduced from M to $\frac{M}{2} + 1$ without any performance loss for each symbol.

Algorithm 1 Low-complexity MIMO detection based on DRSD with ISMMSE-PIC

Initialization: Set $M_T^{ha}, M_T^{so} = 1, \bar{s}_m^{ha} = 0, v_m^{ha} = 1$
$W = (\mathbf{H}^{ha} V^{ha} H^{ha,H} + \sigma^2 I)^{-1} H^{ha}$

Beginning of procedure:

for k=1:1:M **do**
$\mathbf{y}(s_k^{so}) = \mathbf{y} - h_1^{so} s_k^{so}$
for m=1:1:M_T^{ha} **do**
$y_m(s_k^{so}) = \mathbf{y}(s_k^{so}) - \sum_{i=1, i\neq m}^{M_T^{ha}} h_i^{ha} \bar{s}_i^{ha}$
$\mathbf{w} = W_m, \ \check{s}_m^{ha} = \mathbf{w}^H \mathbf{y}_m(s_k^{so})$
$\bar{s}_m^{ha} = argmin \left(\left| \check{s}_m^{ha} - w^H h_m s \right|^2 \right)$
end for
$\hat{\mathbf{s}}^{ha}(s_k^{so}) = \frac{1}{\sigma^2} \left\| \mathbf{y}(s_k^{so}) - \mathbf{H}^{ha} \bar{\mathbf{s}}^{ha}(s_k^{so}) \right\|^2$
end for

Determination of LLR values:

$$L_{1,j}^{so} = \min_{s^{so} \in \mathbf{S}_{1,j}^{so(0)}} \left\{ \frac{1}{\sigma^2} \left\| \mathbf{y}(s^{so}) - \mathbf{H}^{ha} \hat{\mathbf{s}}^{ha}(s^{so}) \right\|^2 \right\} - \min_{s^{so} \in \mathbf{S}_{1,j}^{so(1)}} \left\{ \frac{1}{\sigma^2} \left\| \mathbf{y}(s^{so}) - \mathbf{H}^{ha} \hat{\mathbf{s}}^{ha}(s^{so}) \right\|^2 \right\}$$

$$\check{s}_{min,m}^{ha} = w^H y_m(s_{min}^{so})$$

$$L_{m,j}^{ha} = \min_{s \in \Omega_j^0} \left\{ \frac{1}{\sigma^2} |\check{s}_{min,m}^{ha}(\mathbf{s}_{min}^{so}) - w^H h_m s|^2 \right\} - \min_{\mathbf{s} \in \Omega_j^1} \left\{ \frac{1}{\sigma^2} \left| \check{s}_{min,m}^{ha}(\mathbf{s}_{min}^{so}) - w^H h_m s \right|^2 \right\}$$

IV. COMPLEXITY AND PERFORMANCE EVALUATION

The complexity of the proposed algorithm is compared with that of ISMMSE-PIC detection. The number of visited constellation points for the soft symbols, such as tree searching, and the highest-order term for the hard symbols, such as inverse matrix operation $O(M_T^3)$, are selected as the complexity measure references because they mainly govern the calculation complexity [15] and [21]. In addition, the complexity of the channel decoding is considered because of the dependence of the ISMMSE-PIC detection performance on that of the decoder, which usually uses low data rates for channel coding; the algorithm simply increases the computational complexity of the decoder. Therefore, a 5/6 channel code rate to focus on the analysis of the detection performance and throughput, is only considered. First, with the conventional ML computation complexity, the number of visited nodes is given by:

$$CC_{ML}(M_T) = \sum_{i=1}^{M_T} M^i = \frac{M^{M_T+1} - M}{M - 1}. \tag{35}$$

where CC represents computational complexity. Because the conventional search algorithm visits all the nodes of the tree (which has M^i nodes) in the i-th ($i = 1, 2, \ldots, M_T$) layer.

TABLE 2. Computational complexity for the algorithms.

Algorithm	Computational Complexity
ML	$\frac{M^{M_T+1}-M}{M-1}$
ISMMSE-PIC	$M_T M + {M_T}^3$
DRSD MMSE-PIC	$\lceil \frac{M_T}{M_T^{so}} \rceil (\frac{M^{M_T^{so}+1}-M}{M-1} + M^{M_T^{so}} \cdot M_T^{ha} \cdot M + (M_T^{ha})^3)$
Proposed($M_T^{so}=1$)	$M + M \cdot M_T^{ha} \cdot (\frac{M}{2}+1) + (M_T^{ha})^3$
Proposed($M_T^{so}=3$)	$\lceil \frac{M_T}{3} \rceil (\frac{M^4-M}{M-1} + M^3 \cdot M_T^{ha} \cdot (\frac{M}{2}+1) + (M_T^{ha})^3)$

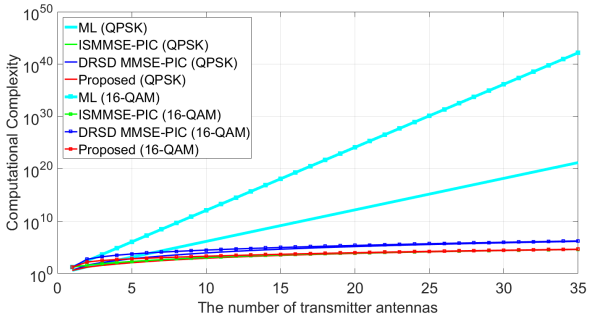

FIGURE 5. Comparison of the computational complexity of the algorithms.

Otherwise, based on DRSD, the number of visited nodes for soft detection of the $M_T^{so}(M_T = M_T^{so} + M_T^{ha})$ symbols is defined as:

$$CC_{DRSD,part}(M_T^{so}, M_T^{ha}) = \frac{M^{M_T^{so}+1} - M}{M-1} + CC_{\text{MMSE-PIC}}(M_T^{so}, M_T^{ha}), \tag{36}$$

where $CC_{\text{MMSE-PIC}}(M_T^{so}, M_T^{ha})$ is the number of visited nodes of the MMSE-PIC detector as well as the highest-order term representing the computational complexity for the calculation. By repeating the same partial DRSD $\lceil M_T/M_T^{so} \rceil$ times for determining the complete LLR values, the total number of visited nodes can be obtained as:

$$CC_{DRSD,total}(M_T^{so}, M_T^{ha}) = \lceil \frac{M_T}{M_T^{so}} \rceil CC_{DRSD,part}(M_T^{so}, M_T^{ha}). \tag{37}$$

The scheme employing hard detection based on MMSE-PIC reduces the number of candidates for tree searching, as implied in (29). To calculate the complexity of the hard detectors, the number of visiting nodes and the highest-order term are calculated as

$$CC_{\text{MMSE-PIC}}(M_T^{so}, M_T^{ha}) \approx M^{M_T^{so}} \cdot M_T^{ha} \cdot M + (M_T^{ha})^3. \tag{38}$$

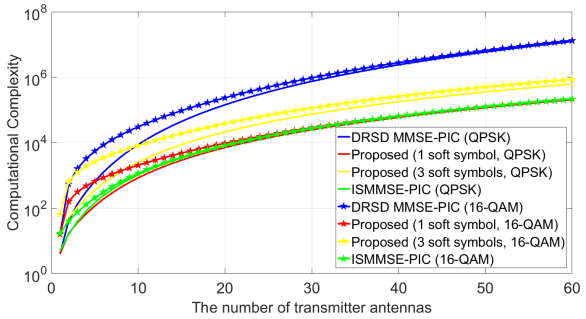

FIGURE 6. Comparison of the computational complexity of the algorithms without using the ML algorithm.

The complexity of DRSD MMSE-PIC is expressed as:

$$CC_{DRSD,total}(M_T^{so}, M_T^{ha}) \approx \lceil M_T/M_T^{so} \rceil \left\{ \frac{M^{M_T^{so}+1} - M}{M-1} + M^{M_T^{so}} \cdot M_T^{ha} \cdot M + (M_T^{ha})^3 \right\}. \tag{39}$$

To calculate the complete LLR values with soft symbols, the MMSE-PIC operation is recursively used, which results in computational complexity higher than that of ISMMSE-PIC. To mitigate the complexity burden, one symbol for soft detection is employed, and LLR^{ha} values with geometric symmetry are utilized. Then, the complexity of the proposed scheme with DRSD MMSE-PIC for one soft symbol and with ISMMSE-PIC for hard symbols is determined as:

$$CC_{Proposed}(M_T^{so}=1, M_T^{ha}) \approx M + M \cdot M_T^{ha} \cdot (\frac{M}{2}+1) + (M_T^{ha})^3. \tag{40}$$

The complexity of ISMMSE-PIC is given by:

$$CC_{ISMMSE-PIC}(M_T) \approx M_T M + {M_T}^3. \tag{41}$$

Table 2 summaries the computational complexity of the ML, ISMMSE-PIC, DRSD MMSE-PIC, and proposed detectors by the complexity measure references [15], [21]. The parameter design M_T^{so} plays a big trade-off role between computational complexity and performance. To present computational complexity of the proposed detectors, the setting of $M_T^{so} = 1$ or $M_T^{so} = 3$ has been established. Repeated use of DRSD MMSE-PIC increases its complexity by $\lceil M_T/M_T^{so} \rceil$ times from its initial complexity value. The complexity of the proposed scheme, with the cube of the number of hard symbols, such as $M_T - 1$ has lower computational complexity than ISMMSE-PIC because of the cube of the number of symbols such as M_T. However, the proposed scheme should be repeatedly calculated for each constellation point, indicating that the proposed scheme and ISMMSE-PIC exhibit similar computational complexities. In addition, the ML detector is not feasible for large-scale or massive MIMO systems owing to the term M^{M_T}. Fig. 5 compares the computational complexity of the algorithms with QPSK and 16-QAM, respectively. The ML detector shows extremely high computational complexity, which

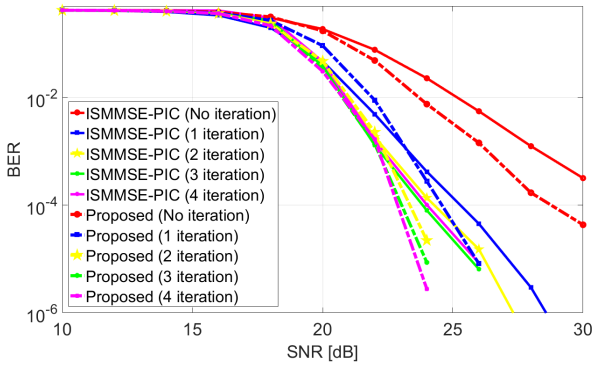

FIGURE 7. The proposed detector ($M_T^{so} = 1$) BER curves for 16-QAM with ten transmitter and receiver antennas.

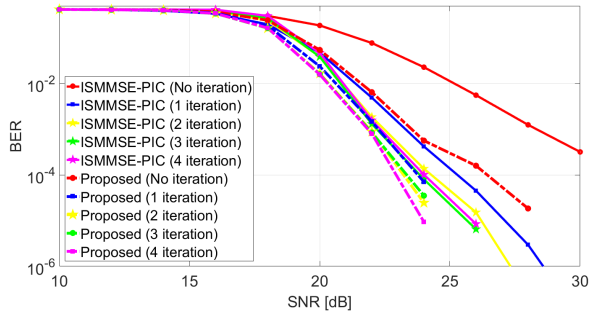

FIGURE 8. The proposed detector ($M_T^{so} = 3$) BER curves for 16-QAM with ten transmitter and receiver antennas.

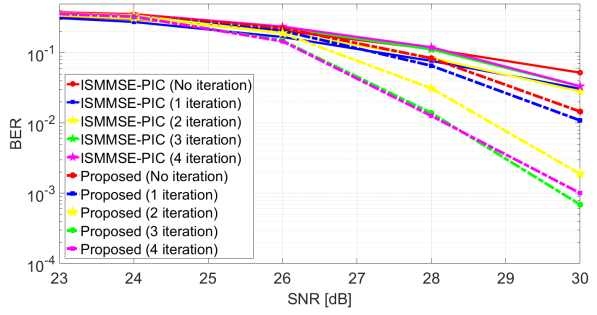

FIGURE 9. The proposed detector ($M_T^{so} = 1$) BER curves for 64-QAM with ten transmitter and receiver antennas.

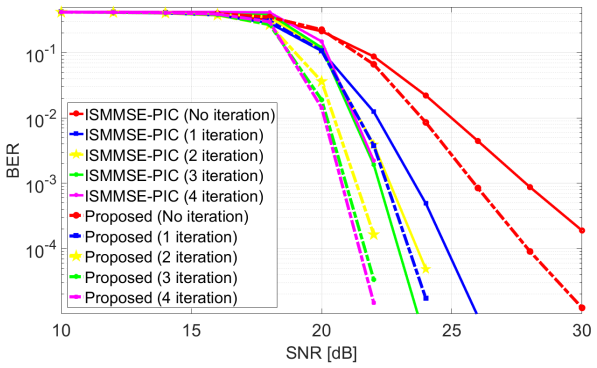

FIGURE 10. The proposed detector ($M_T^{so} = 1$) BER curves for 16-QAM with 20 transmitter and receiver antennas.

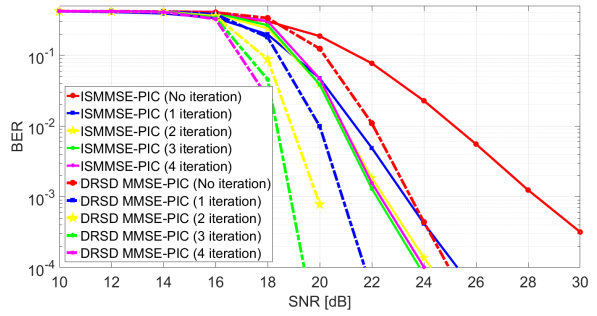

FIGURE 11. DRSD MMSE-PIC for all transmitted symbols BER curves for 16-QAM with 10 transmitter and receiver antennas.

increases exponentially with M_T. Fig. 6 compares the computational complexity of algorithms with QPSK and 16-QAM, without the ML algorithm. The proposed ($M_T^{so} = 1$) and ISMMSE-PIC detectors exhibit similar computational complexities, which increase exponentially with M_T.

The performance of the proposed scheme in a MIMO-OFDM system with $M_T = M_R = 10$ or 20 for 16-QAM and 64-QAM constellations is evaluated. The simulation results are based on a convolution encoder (code rate: 5/6, constraint length: 7, polynomials [133 171]) and are obtained using the Bahl–Cocke-Jelinek–Raviv channel decoder [16] based on the min-sum algorithm. It is commonly implemented for iterative operation algorithms. The strength of the decoder lies in its ability to consider both past and future bits. A 3-tap uniform channel model is used for the practical performance comparison. One packet consists of four OFDM symbols, and 128 subcarriers are used for the simulation. Five outer iterations are considered because of the simulation time limitation, and the simulations are conducted over 1,000 packets with different SNR values.

Fig. 7 shows the bit error rate (BER) curves for 16-QAM with $M_T = M_R = 10$. The number of soft demodulation symbols is selected as $M_T^{so} = 1$. The proposed scheme performs better than ISMMSE-PIC, which initially exhibits performance degradation without a priori information. Because of solving the initial poor performance problem, the scheme's performance with iterations also enhances. Especially, high BER curves are obtained under high SNR conditions. Fig. 8 shows the BER curves for 16-QAM with 10 transmitter and receiver antennas ($M_T = M_R = 10$) and three soft symbols ($M_T^{so} = 3$). The proposed algorithm with $M_T^{so} = 3$ demonstrates better BER performance compared to the previously scheme with $M_T^{so} = 1$. However, as shown in Fig. 6, the computational complexity of the algorithm ($M_T^{so} = 3$) is higher than the scheme with $M_T^{so} = 1$. The BER performance for 64-QAM is plotted in Fig. 9; the tendency is similar to that of the 16-QAM case. However,

the difference between the performances amplifies with the increasing SNR for higher-order modulation. Fig. 10 shows the BER curves for 16-QAM with 20 transmitter and receiver antennas ($M_T = M_R = 20$) and one soft symbol ($M_T^{so} = 1$). Evidently, the proposed scheme shows the same performance as that depicted in Fig 7. Fig. 11 shows the BER curves for 16-QAM with 10 transmitter and receiver antennas ($M_T = M_R = 10$), and the complete LLR values, which are calculated via repeated DRSD MMSE-PIC ($M_T^{so} = 1$), for the transmitter symbols ($M_T = 10$) are shown as well. These results indicate that the SNR performance of the proposed scheme is higher than that of the others. However, it results in high computational complexity, and the detection algorithm depending on the channel and SNR conditions can be chosen. In conclusion, the proposed scheme and DRSD MMSE-PIC detector can provide a trade-off between computational complexity and performance.

V. CONCLUSION

Herein, we proposed a low-complexity MIMO detection method based on DRSD with ISMMSE-PIC. The DRSD-based strategy was presented to enhance detection performance. The proposed scheme for the rest of the symbols directly incorporated the ISMMSE-PIC detection method with the geometric symmetry property to reduce computational complexity. Through simulations and computational complexity analysis, it has been demonstrated that our proposed detector achieves superior performance compared to the ISMMSE-PIC method, while maintaining comparable levels of complexity. The detector can provide a trade-off between computational complexity and performance for MIMO detection and overcomes the dependence on decoder performance, unlike ISMMSE-PIC. The scheme is an effective ISMMSE-PIC-based detection strategy for large-scale MIMO or massive MIMO systems. As an extension of this work, we will implement massive MIMO FPGA prototype and evaluate proposed algorithm in practical MIMO systems in the future.

ACKNOWLEDGMENT

The authors would like to thank C. Studer for providing the basic software package that contained the ISMMSE-PIC algorithm for the simulations.

REFERENCES

[1] M. A. Albreem, M. Juntti, and S. Shahabuddin, "Massive MIMO detection techniques: A survey," *IEEE Commun. Surveys Tuts.*, vol. 21, no. 4, pp. 3109–3132, 4th Quart., 2019.

[2] M. Pappa, C. Ramesh, and M. N. Kumar, "Performance comparison of massive MIMO and conventional MIMO using channel parameters," in *Proc. Int. Conf. Wireless Commun., Signal Process. Netw. (WiSPNET)*, Mar. 2017, pp. 1808–1812.

[3] P. Patcharamaneepakorn, S. Wu, C.-X. Wang, e. M. Aggoune, M. M. Alwakeel, X. Ge, and M. D. Renzo, "Spectral, energy, and economic efficiency of 5G multicell massive MIMO systems with generalized spatial modulation," *IEEE Trans. Veh. Technol.*, vol. 65, no. 12, pp. 9715–9731, Dec. 2016.

[4] E. Björnson, E. G. Larsson, and M. Debbah, "Massive MIMO for maximal spectral efficiency: How many users and pilots should be allocated?" *IEEE Trans. Wireless Commun.*, vol. 15, no. 2, pp. 1293–1308, Feb. 2016.

[5] *NR; Physical Channel, Modulation, 3rd Generation Partnership Project, Technical Specification Group, Radio Access Network*, document TS 38.211, V15.4.0 Release 15, 3GPP, 2018.

[6] X. Jing, J. Wen, and H. Liu, "Low-complexity soft-output signal detector for massive MIMO with higher order QAM constellations," *Digit. Signal Process.*, vol. 108, Jan. 2021, Art. no. 102886.

[7] M. Kim, S. Mandrá, D. Venturelli, and K. Jamieson, "Physics-inspired heuristics for soft MIMO detection in 5G new radio and beyond," in *Proc. 27th Annu. Int. Conf. Mobile Comput. Netw.*, Sep. 2021, pp. 42–55.

[8] Y. Jiang, M. K. Varanasi, and J. Li, "Performance analysis of ZF and MMSE equalizers for MIMO systems: An in-depth study of the high SNR regime," *IEEE Trans. Inf. Theory*, vol. 57, no. 4, pp. 2008–2026, Apr. 2011.

[9] S. Yang and L. Hanzo, "Fifty years of MIMO detection: The road to large-scale MIMOs," *IEEE Commun. Surveys Tuts.*, vol. 17, no. 4, pp. 1941–1988, 4th Quart., 2015.

[10] R. Mahmoudi and K. Iniewski, "Chapter 8: Efficient MIMO receiver design for next generation wireless systems," in *Low Power Emerging Wireless Technologies*. Boca Raton, FL, USA: CRC Press, 2013.

[11] B. M. Hochwald and S. T. Brink, "Achieving near-capacity on a multiple-antenna channel," *IEEE Trans. Commun.*, vol. 51, no. 3, pp. 389–399, Mar. 2003.

[12] L. G. Baro and J. S. Thompson, "A fixed-complexity sphere decoder to obtain likelihood information for Turbo-MIMO systems," *IEEE Trans. Emerg. Telecommun. Technol*, vol. 57, no. 5, pp. 2804–2814, 2008.

[13] C. Studer and H. Bölcskei, "Soft–input soft–output single tree-search sphere decoding," *IEEE Trans. Inf. Theory*, vol. 56, no. 10, pp. 4827–4842, Oct. 2010.

[14] J.-W. Choi, J. Lee, H.-L. Lou, and J. Park, "Improved MIMO SIC detection exploiting ML criterion," in *Proc. IEEE Veh. Technol. Conf. (VTC Fall)*, Sep. 2011, pp. 1–5.

[15] S. Shin, H. Choi, J. Jang, and J. Choi, "A low-complexity iterative MIMO detection and decoding scheme using dimension reduction," *Trans. Emerg. Telecommun. Technol.*, vol. 27, no. 1, pp. 136–145, Jan. 2016.

[16] T. L. Narasimhan and A. Chockalingam, "Channel hardening-exploiting message passing (CHEMP) receiver in large-scale MIMO systems," *IEEE J. Sel. Topics Signal Process.*, vol. 8, no. 5, pp. 847–860, Oct. 2014.

[17] H. Prabhu, J. Rodrigues, O. Edfors, and F. Rusek, "Approximative matrix inverse computations for very-large MIMO and applications to linear pre-coding systems," in *Proc. IEEE Wireless Commun. Netw. Conf. (WCNC)*, Apr. 2013, pp. 2710–2715.

[18] B. Kang, J.-H. Yoon, and J. Park, "Low complexity massive MIMO detection architecture based on Neumann method," in *Proc. Int. SoC Design Conf. (ISOCC)*, Nov. 2015, pp. 293–294.

[19] L. Fang, L. Xu, and D. D. Huang, "Low complexity iterative MMSE-PIC detection for medium-size massive MIMO," *IEEE Wireless Commun. Lett.*, vol. 5, no. 1, pp. 108–111, Feb. 2016.

[20] C. Studer, S. Fateh, and D. Seethaler, "ASIC implementation of soft-input soft-output MIMO detection using MMSE parallel interference cancellation," *IEEE J. Solid-State Circuits*, vol. 46, no. 7, pp. 1754–1765, Jul. 2011.

[21] S. Park, "Low-complexity LMMSE-based iterative soft interference cancellation for MIMO systems," *IEEE Trans. Signal Process.*, vol. 70, pp. 1890–1899, 2022.

[22] B. Cheng, Y. Shen, H. Wang, Z. Zhang, X. You, and C. Zhang, "Efficient MMSE-PIC detection for polar-coded system using tree-structured gray codes," *IEEE Wireless Commun. Lett.*, vol. 11, no. 7, pp. 1310–1314, Jul. 2022.

[23] H. J. Park and J. W. Lee, "Design of LDPC coded multi-user massive MIMO systems with MMSE-based iterative joint detection and decoding," *IEEE Access*, vol. 11, pp. 125492–125510, 2023.

[24] S. Fateh, C. Studer, and D. Seethaler, "VLSI implementation of soft-input soft-output MMSE parallel interference cancellation," M.S. thesis, ETH Zurich, Zurich, Switzerland, 2009.

[25] Q. Wang, Q. Xie, Z. Wang, S. Chen, and L. Hanzo, "A universal low-complexity symbol-to-bit soft demapper," *IEEE Trans. Veh. Technol.*, vol. 63, no. 1, pp. 119–130, Jan. 2014.

[26] I.-W. Kang, J.-W. Shin, and H.-N. Kim, "Low-complexity LLR calculation for gray-coded PAM modulation," *IEEE Commun. Lett.*, vol. 20, no. 4, pp. 688–691, Apr. 2016.

SANG-SIK SHIN received the B.S. degree in electronics engineering from Dong-A University, Busan, South Korea, in 2006, and the M.S. degree in information and communication engineering from Daegu Gyeongbuk Institute of Science and Technology (DGIST), Daegu, South Korea, in 2013. He is currently pursuing the Ph.D. degree in electrical and electronics engineering from Pusan National University, Busan, South Korea. From 2005 to 2010, he was with Samsung Electronics Inc., Gumi, South Korea, and developed GSM cellphones for the European market. In 2013, he joined the Defense Agency for Technology and Quality, Jinju, South Korea, where he is currently a Senior Researcher. His research interests include digital signal processing and communications, adaptive filtering, biomedical signal processing, and in particular, signal processing for detection.

HO JAE KIM (Member, IEEE) received the B.S., M.S., and Ph.D. degrees in electronic and electrical engineering from Pusan National University, Busan, South Korea, in 2015, 2017, and 2024, respectively, where he is currently pursuing the integrated Postdoctoral degree in electrical and electronics engineering. His main research interests include digital signal processing, digital communications, array signal processing, and radar and sensor signal processing.

HYOUNG-NAM KIM (Member, IEEE) received the B.S., M.S., and Ph.D. degrees in electronic and electrical engineering from Pohang University of Science and Technology, Pohang, South Korea, in 1993, 1995, and 2000, respectively. From 2000 to 2003, he was with the Electronics and Telecommunications Research Institute, Daejeon, South Korea, developing advanced transmission and reception technology for terrestrial digital television. In 2003, he joined as a Faculty Member with the Department of Electronics Engineering, Pusan National University, Busan, South Korea, where he is currently a full-time Professor. From 2009 to 2010, he was with the Department of Biomedical Engineering, The Johns Hopkins University School of Medicine, as a Visiting Scholar. From 2015 to 2016, he was a Visiting Professor with the School of Electronics and Computer Engineering, University of Southampton, U.K. His research interests include radar/sonar signal processing, machine learning, adaptive filtering, biomedical signal processing, digital communications, electronic warfare support systems, and brain–computer interfaces. He is a member of IEIE and KICS.